

## **Application of a physically-based numerical model of surface and subsurface water flow and solute transport**

**J. E. VANDERKWAAK**

*Department of Geological and Environmental Sciences, Stanford University, Stanford, California 94305, USA*

e-mail: [kwaak@pangea.stanford.edu](mailto:kwaak@pangea.stanford.edu)

**E. A. SUDICKY**

*Department of Earth Sciences, University of Waterloo, Waterloo, Ontario N2L 3G1, Canada*

**Abstract** A fully-integrated numerical model is presented which considers the flow of water and transport of multiple solutes on the two-dimensional land surface and in the three-dimensional, dual-continua subsurface, under variably-saturated conditions. Linkage between the various continua is through first-order, physically based flux relationships or through pressure head and concentration continuity assumptions. Full coupling of flow and transport is achieved by assembling and solving one system of discrete algebraic equations such that water and solute fluxes between continua are determined simultaneously. To achieve a high degree of computational efficiency, robust and efficient discretization and solution techniques are utilized. The numerical model was tested by simulating a controlled field experiment described by Abdul & Gillham (1989) involving coupled surface–subsurface flow and tracer transport in a small subcatchment at CFB Borden, Ontario. Observed surface discharge volumes and timings arising from the application of artificial rainfall containing a tracer were simulated with reasonable accuracy using published or measured parameter values and minimal calibration. The observed dynamic response is shown to be a nonlinear function of surface and subsurface flow processes that are affected by subsurface permeability, surface roughness, topography, and initial conditions. Excess rainfall and groundwater seepage that flows overland initially, generate surface ponding within microtopographic depressions, including those located in the initially dry stream channel. The ponded surface water forms an internal, transient constraint on the porous medium pressure head near the land surface which is not reflected in solutions making use of traditional seepage face algorithms. The dominant streamflow mechanism deduced from the simulations is infiltration excess over an increasing contributing area, with the contributing area controlled by rapid response of the capillary fringe. Water originating above the initial water table overshadows groundwater contributions in this case.

### **SUMMARY OF THE FIELD EXPERIMENT**

The field-scale experiments of Abdul & Gillham (1989) were conducted at Canadian Forces Base Borden, located north of Toronto, Ontario, Canada. The area selected for the experiment is described as being grass covered and approximately 18 by 90 m in plan view (Fig. 1). A man-made stream channel, which is grass-free and approximately 60 cm wide, is located approximately 1.2 m below the surrounding topographic highs. The underlying porous medium consists of an organic-rich sandy layer, approximately

10 to 20 cm thick, overlying sand containing small-scale interbeds with occasional silty layers and lenses (Sudicky, 1986). A thick deposit of clayey silt underlies the aquifer at a depth of about four metres (Akindunni & Gillham, 1992). The measured characteristic saturation-pressure relationship (Abdul, 1985) indicates that the sand is saturated for a distance of about 30 cm above the water.

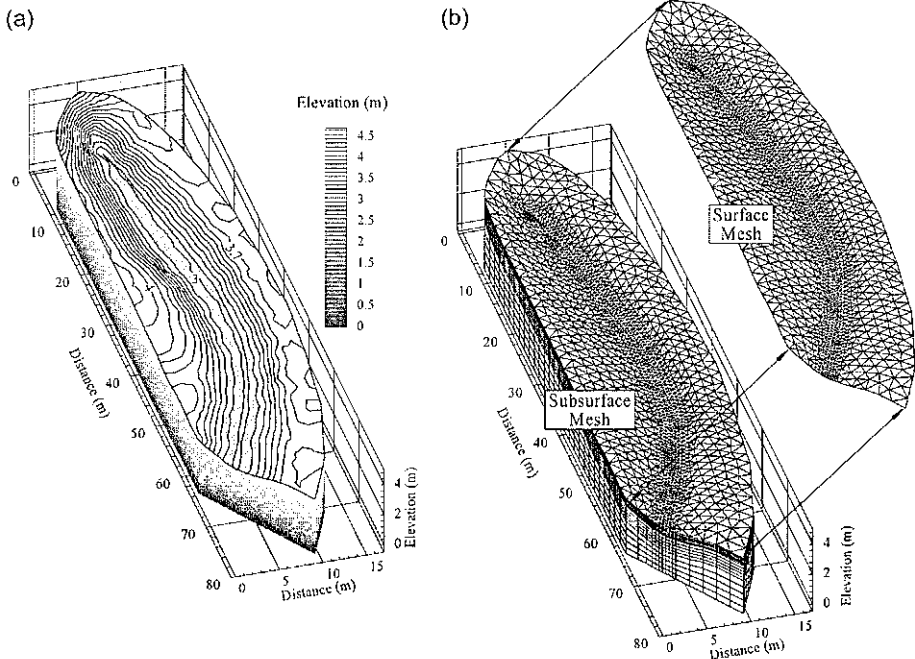


Fig. 1 Illustration of (a) surface topography of the site of the Borden rainfall-runoff field experiment (after Abdul, 1985), and (b) finite element meshes utilized in field-scale coupled surface-subsurface simulations (after VanderKwaak, 1999).

For the experiment under consideration, the initial water table lies about 22 cm below the streambed, indicating that the capillary fringe extends to the land surface along and adjacent to the stream. Abdul (1985) applied artificial rainfall for 50 min at a rate of  $2.0 \text{ cm h}^{-1}$ , observing a rapid rise of the water table and both overland and stream flow. The rainfall contained bromide, providing a conservative tracer to differentiate “event” and “pre-event” water (Fig. 2). The interpreted streamflow generation mechanisms were: (a) increased overland flow due to rainfall excess onto regions of saturated sand, and (b) groundwater discharge due to increased subsurface hydraulic head gradients. Groundwater or pre-event contributions were interpreted as forming up to 37% of streamflow, based both on chemically based hydrograph separations and on groundwater discharge volumes (seepage) calculated using flow nets.

## SUMMARY OF THE NUMERICAL MODEL

The numerical model utilized in this work describes the flow of water and transport of solutes in three separate continua: within the porous medium, the fractures/macropores

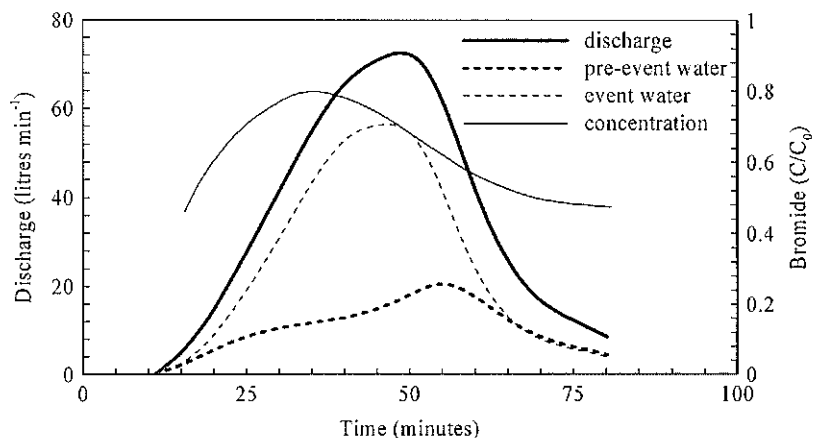
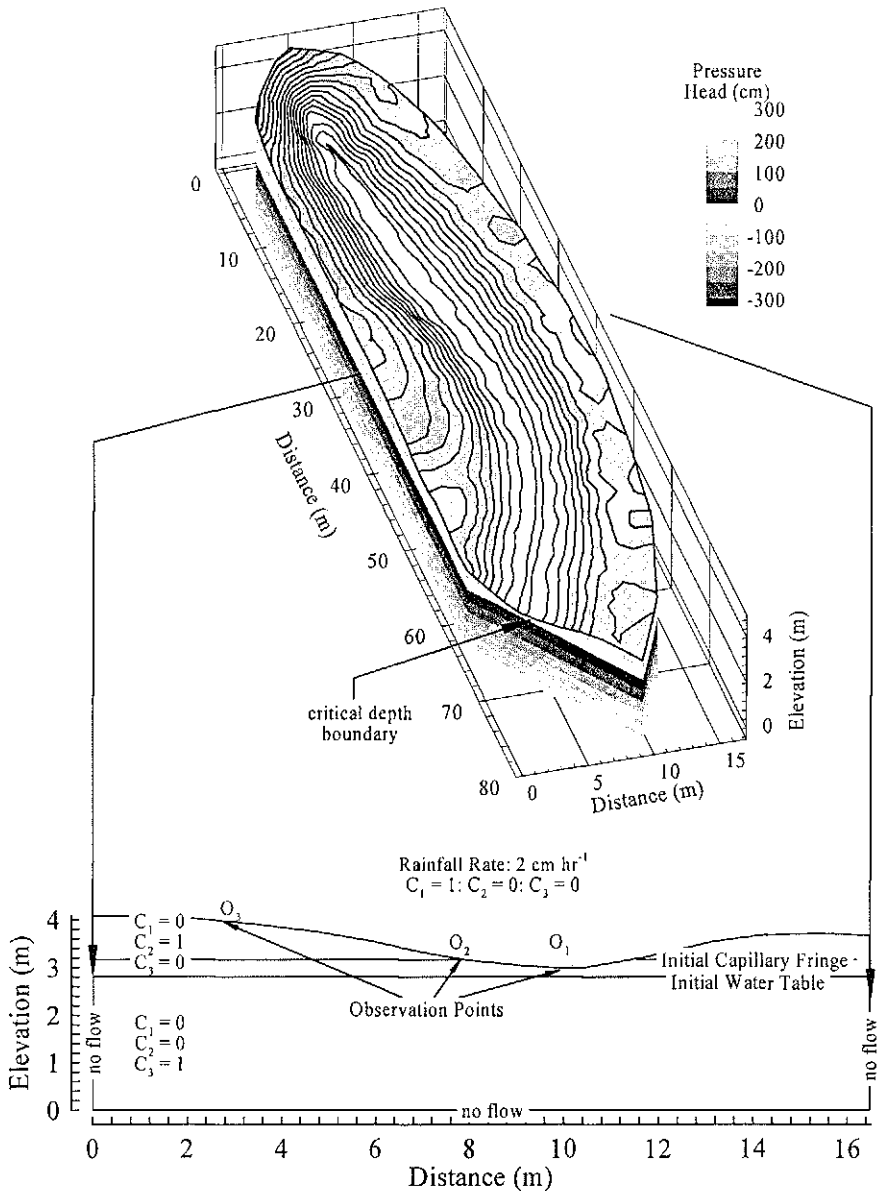


Fig. 2 Measured discharge volumes, normalized tracer concentrations and hydrograph separation for the Borden field experiment (after Abdul, 1985).

and on the land surface. The two-dimensional diffusion-wave equation is implemented to describe overland flow in shallow surface water while flow in variably-saturated porous media and macropores was described by the three-dimensional Richards' equation. Transport in both the surface and subsurface systems is described by advection–dispersion equations. Coupling of surface and subsurface flow and transport is achieved by assembling and solving one system of discrete algebraic equations so that water and solute fluxes between continua are determined as part of the solution. Linkage is through the assumption of primary variable continuity or via first-order, physically based flux relationships. Water and solute exchange between continua is assumed to be described by one-dimensional Darcy and advection–dispersion equations, respectively. Flow and transport coupling coefficients are defined as functions of characteristic length scales of interaction, fluid or solute properties, and system parameters such as saturation or permeability. Use of large exchange coefficient values promotes concentration and pressure head continuity between two interacting continua, and small values promote disequilibrium.

The numerical model is modular in form, is tailored towards irregular geological, surficial and areal geometries, and utilizes robust and efficient discretization and solution techniques. The governing flow and transport equations are discretized in space using the control volume finite element (CVFE) method, allowing a consistent interpretation of flow and transport processes both within and between continua. The CVFE method combines the geometric flexibility of finite elements with the local conservation characteristics of control volumes. Simple element types are utilized to allow the efficient use of influence coefficients in the evaluation of spatial integrals. Element types can be spatially variable, a useful option in simulations combining complex geological and topographical geometries. Each node in the finite element mesh may have multiple unknowns, with each unknown associated with different continua. Nonlinear flux limiters are utilized in solving advective–dispersive transport to minimize numerical dispersion. The discrete flow equations are linearized using Newton's method and numerical derivatives are utilized to efficiently construct both

the flow and transport Jacobians. The convergence of the flow Newton iterations is enhanced by primary variable switching. Adaptive temporal-weighting algorithms are utilized for both flow and transport. The systems of nonlinear equations are solved in a fully coupled fashion so that fluid and solute exchanges and nonlinear boundary conditions are determined as part of the iterative solution. Approximate solutions to the linearized equations are generated using an iterative sparse-matrix solver. Further details regarding the numerical model may be found in VanderKwaak (1999) and VanderKwaak *et al.* (1999a).



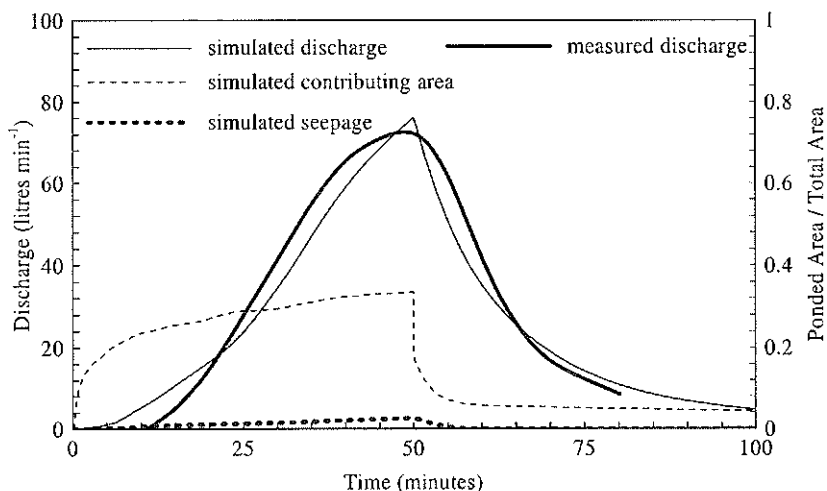
**Fig. 3** Illustration of initial and boundary conditions for field-scale first-order-coupled surface–subsurface simulations, and the locations of three observation points.

## DISCRETIZATION AND MODEL INPUT PARAMETERS

The finite element meshes utilized in the three-dimensional field-scale simulations are presented in Fig. 1(b). Vertical discretization is on the order of 1 cm adjacent to the land surface, increasing to about 1 m at depth. Horizontal discretization is on the order of 20 cm in and adjacent to the stream channel, increasing to about 1 m on the topographic highs. Boundary and initial conditions are presented in Fig. 3 for simulations of first-order coupled surface–subsurface flow and transport. Rainfall is applied to the surface equations for 50 min at a rate of 2 cm h<sup>-1</sup>, followed by 50 min of drainage. Critical depth conditions are utilized at the stream outflow, representing the weir used in the field experiment. No additional boundary conditions are specified. Although a single tracer was applied in the field experiment, three tracers are utilized in the simulations to allow differentiation of rainfall from water originating above and below the initial water table. Parameters for all simulations are derived from measured or published values and a limited sensitivity analysis (see VanderKwaak, 1999; VanderKwaak & Sudicky, 1999a,b).

## SIMULATED RAINFALL-RUNOFF RESPONSE

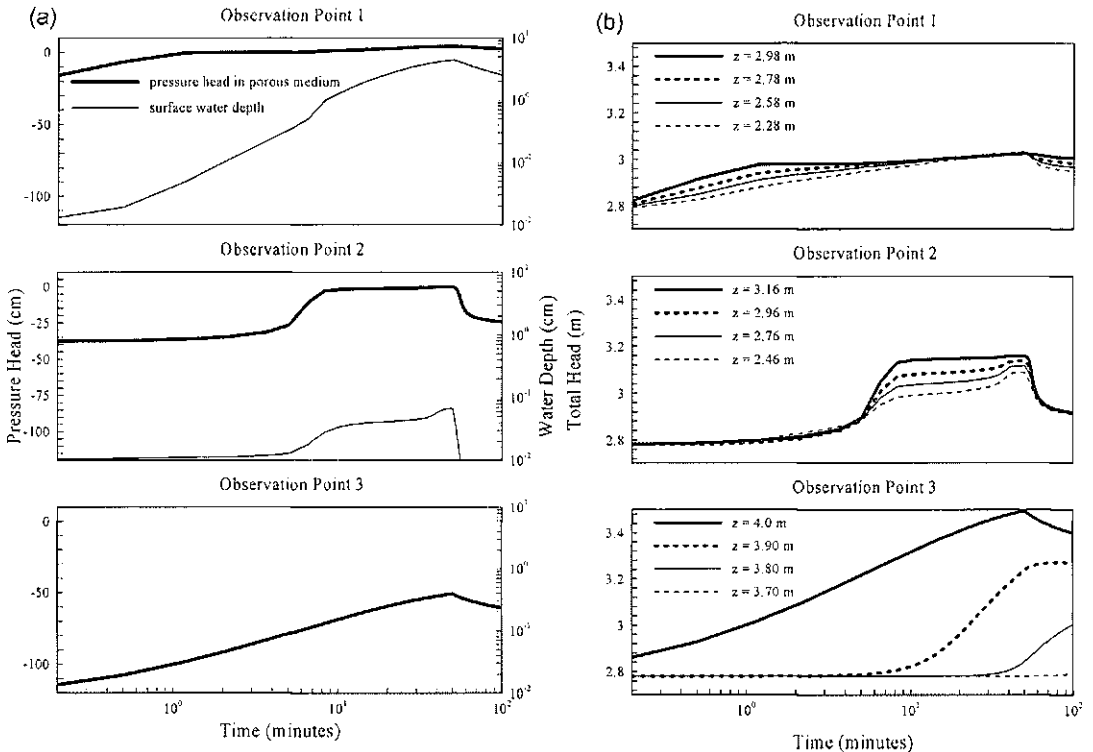
A comparison of the measured stream discharge with that predicted with the coupled surface–subsurface numerical model is presented in Fig. 4. The simulated hydrograph slightly overpredicts both early-time response and peak discharge, while reproducing both the time to peak and the recession portions of the measured hydrograph with reasonable accuracy. Simulated groundwater (seepage) contributions to streamflow are shown to be small. Also presented in Fig. 4 is the approximate area of the land surface contributing to stream flow via overland flow. This area is calculated by dividing the ponded area of the land surface by the total surface area. The figure indicates that, while



**Fig. 4** Comparison of measured and simulated stream discharges vs time (hydrographs) and the illustration of the simulated area contributing water to the stream via overland flow.

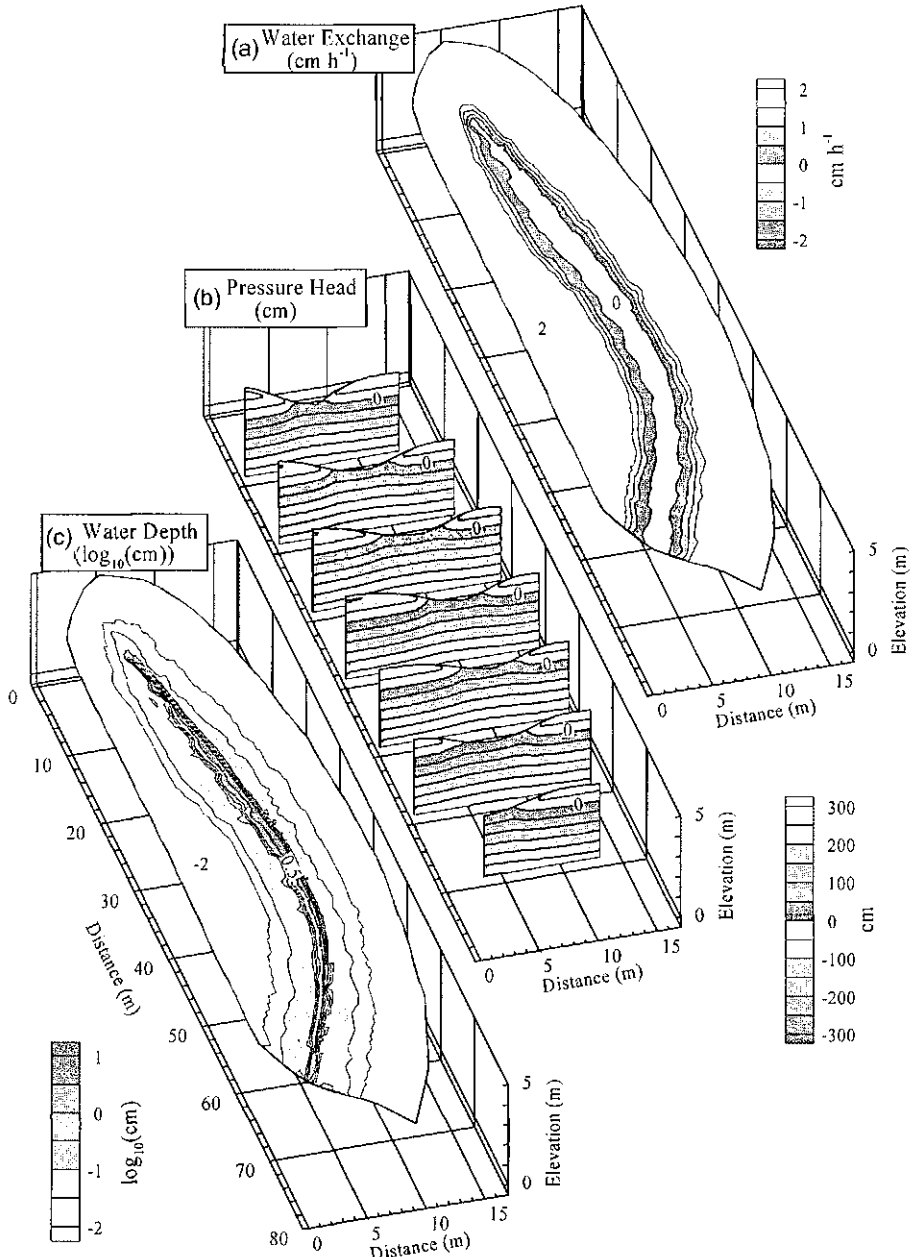
increased surface discharge correlates with increased surface ponding, the relationship between surface discharge and contributing area is nonlinear. Simulated contributing areas increase more rapidly than stream discharge at early time (i.e. less than about 15 min), while decreasing more rapidly than stream discharge when rainfall ceases. This nonlinearity results from the relationship between water depth and velocity embedded in the Manning equation, and by the spatially- and temporally-variable storage and infiltration capacities of the porous medium, which acts as a source/sink term for the surface water continuum.

Figure 5(a) presents graphs of pressure head and water depth versus time for three observation points located on the land surface along a cross section at  $x = 40$  m. These observation points correspond to the streambed, the valley bottom, and the upland region, respectively (see Fig. 3). High initial saturation and reduced storage capacity beneath and adjacent to the stream channel cause a rapid change of negative pressure heads to positive values. Water depths in the stream rise to about 5 cm at peak discharge, decreasing slowly during recession. Water depths are smaller on the slopes adjacent to the stream, and decrease rapidly following the end of the rainfall event. Pressure head values remain negative at the upland observation point as initial saturations are close to residual values and significant storage capacity exists in the porous medium.



**Fig. 5** Graphs of (a) pressure head and water depth vs time, and (b) total head vs time and elevation at three locations on the land surface. Observation point one is located at the stream, observation point two is located adjacent to the stream, and observation point three is located in the upland region (see Fig. 3).

Total head gradients beneath the stream (Fig. 5(b)) indicate infiltration into the streambed for about 5 min, corresponding to the delay in surface discharge initiation and the time required to occupy the small storage capacity of the capillary fringe. Hydraulic head gradients adjacent to the stream indicate infiltration for the duration of the simulation, with vertical gradients decreasing after about the first 20 min. Not all



**Fig. 6** Summary of first-order-coupled flow solution at 50 minutes: (a) rate of water exchange between the porous medium and surface equations, (b) pressure head in porous medium, and (c) surface water depth.

rainfall enters the porous medium at this location, but instead contributes to overland and stream flow as a function of spatially and temporally variable infiltration rates. Surface discharge timing and volume, therefore, are intimately related to the storage capacity and hydraulic conductivity of the porous medium. Head gradients beneath the uppermost observation point indicate infiltrating conditions for the duration of the simulation, with the wetting front penetrating to a depth of about 40 cm at the end of the rainfall event.

Figure 6 presents a summary of the coupled flow solution at 50 min, corresponding to both the end of the rainfall event and the time of peak surface water discharge. The rate of water exchange between continua (Fig. 6(a)), pressure head contours on seven cross-sections (Fig. 6(b)), and contours of surface water depth on the land surface (Fig. 6(c)) are depicted. Seepage is largest at the toe of the slopes where the rapid response of the water table interacts with topography to generate complex subsurface flow. Surface ponding in the stream channel, where depths have risen to about 5 cm, is reflected in decreased seepage along the channel axis. Surface water depths adjacent to the stream have also risen, subtly altering the spatial distribution of infiltration and groundwater discharge by filling small depressions in the land surface topography. The flow simulation indicates that groundwater discharge accounts for less than 5% of total surface water discharge.

## CONCLUSIONS

The set of simulations based upon the field experiment performed by Abdul (1985) clarifies the role of the capillary fringe on streamflow generation in the relatively homogeneous sand underlying CFB Borden. The coupled surface–subsurface flow model is able to reproduce the observed rapid water table response and resulting overland and stream flow. Observed surface discharge volumes and timing were simulated with reasonable accuracy using published or measured parameter values and minimal calibration. The simulated response of the capillary fringe to rainfall is consistent with both theory (Gillham, 1985) and observations (Abdul, 1985; Abdul & Gillham, 1989). The simulations suggest that, while the low storage capacity of the capillary fringe is clearly responsible for the observed rapid hydrological response, increased subsurface head gradients do not cause significant groundwater seepage. Rather, infiltration rates along the stream axis are reduced, with runoff formed largely by excess rainfall over a dynamic contributing area (e.g. Dunne & Black, 1970). Although not shown here, the coupled surface–subsurface transport simulations suggest that rainfall tracer dilution occurs largely by diffusive processes as water flows over the land surface to the stream, over relatively short flow paths, and subsequently down the stream channel. Tracer originating above the initial water table enters the surface water by similar processes, augmenting the small volumes of seepage (advective transport) caused by increased subsurface hydraulic gradients.

## REFERENCES

- Abdul, A. S. (1985) Experimental and numerical studies of the effect of the capillary fringe on streamflow generation. PhD Thesis, University of Waterloo, Waterloo, Ontario, Canada.

- Abdul, A. S. & Gillham, R. W. (1989) Field studies of the effects of the capillary fringe on streamflow generation. *J. Hydrol.* **112**, 1–18.
- Akindunni, F. F. & Gillham, R. W. (1992) Unsaturated and saturated flow in response to pumping of an unconfined aquifer: numerical investigation of delayed drainage. *Ground Water* **30**(6), 873–884.
- Dunne, T. & Black, R. D. (1970) An experimental investigation of runoff prediction in permeable soils. *Wat. Resour. Res.* **6**, 478–490.
- Gillham, R. W. (1985) The capillary fringe and its effect on water-table response. *J. Hydrol.* **67**(4), 307–324.
- Sudicky, E. A. (1986) A natural gradient experiment on solute transport in a sand aquifer; spatial variability of hydraulic conductivity and its role in the dispersion process. *Wat. Resour. Res.* **22**(13), 2069–2082.
- VanderKwaak, J. E. (1999) Numerical simulation of flow and chemical transport in integrated surface-subsurface hydrologic systems. PhD Thesis, Department of Earth Sciences, University of Waterloo, Waterloo, Ontario, Canada.
- VanderKwaak, J. E., Sudicky, E. A. & Forsyth, P. A. (1999) An integrated numerical model of flow and transport in coupled surface-subsurface hydrologic systems. 1: Theoretical development and solution methods. For submission to *Adv. Wat. Res.*
- VanderKwaak, J. E. & Sudicky, E. A. (1999a) An integrated numerical model of flow and transport in coupled surface-subsurface hydrologic systems. 2: Simulation of a laboratory-scale rainfall-runoff and tracer transport experiment. For submission to *Adv. Water Res.*
- VanderKwaak, J. E. & Sudicky, E. A. (1999b) An integrated numerical model of flow and transport in coupled surface-subsurface hydrologic systems 3: Simulation of a field-scale rainfall-runoff and tracer transport experiment. For submission to *Adv. Wat. Res.*